

# Computational Study of Ion Binding to the Liquid Interface of Water<sup>†</sup>

Liem X. Dang

*Environmental Molecular Sciences Laboratory, Pacific Northwest National Laboratory,  
Richland, Washington 99352*

*Received: August 12, 2002*

We have performed extensive classical molecular dynamics simulations to examine the molecular transport mechanisms of  $\text{I}^-$ ,  $\text{Br}^-$ ,  $\text{Cl}^-$ , and  $\text{Na}^+$  ions across the liquid/vapor interface of water. The potentials of mean force were calculated using the constrained mean force approach and polarizable potential models were used to describe the interactions among the species. The simulated potentials of mean force were found to be different, depending on the type of anion. The larger  $\text{I}^-$  and  $\text{Br}^-$  anions bind more strongly to the liquid/vapor interface of water than that of the smaller  $\text{Cl}^-$  ion. It is important to note that most of the gas phase and solution phase properties of the  $\text{Br}^-$  anion are quite similar to that of the  $\text{Cl}^-$  ion. At the interface, however, the interactions of the  $\text{Br}^-$  and  $\text{Cl}^-$  anions with the water interface appeared to be significantly different. We found that the anions approach the interface more closely than cations. We have also studied the transport mechanism of an  $\text{I}^-$  across the water/dichloromethane interface. The computed potential of mean force showed no well-defined minimum as in the liquid/vapor case, but a stabilization free energy of about  $-1$  kcal/mol near the interface with respect to the bulk liquid was observed. The  $\text{I}^-$  anion carried a water molecule with it as it crossed the interface. This result is in agreement with a recent experimental study on a similar system. Our work differs from earlier contributions in that our potential models have taken many-body effects into account, and in some cases, these effects cannot be neglected.

## I. Introduction

The adsorption and distribution of ions at interfaces is a fundamental process encountered in a wide range of biological and chemical systems.<sup>1–3</sup> In particular, the manner in which water molecules solvate ions is relevant to chemical and physical processes such as chemical reactions at the interface. The structure and stability of large molecules and membranes depend on the distribution of ions and/or counterions. The ion transport mechanism can be an important factor in atmospheric processes such as molecular uptake of ions at the air/liquid interface,<sup>4</sup> and to environmental problems such as the interaction of contaminated organic solvents in groundwater and separation chemistry performed in binary solvent systems.<sup>5</sup>

Considerable progress has been made during the past decade in understanding the equilibrium properties of ion solvation at the liquid interfaces of water. This includes the work of Wilson and Pohorille on transferring monovalent ions ( $\text{Cl}^-$ ,  $\text{F}^-$  and  $\text{Na}^+$ ) across a water liquid/vapor interface.<sup>6</sup> This study indicated that less energy is required to transport the anion across the interface than to transport the cation. In addition, they found that there is no difference between the computed free-energy profiles of the ions  $\text{Cl}^-$  and  $\text{F}^-$ . Benjamin and co-workers have contributed a great deal to our understanding of the ion transport mechanisms across liquid water interfaces.<sup>7</sup> They studied and proposed transport mechanisms for the  $\text{Cl}^-$  anion and TMA across the liquid–liquid interface. Recently, Tobias and co-workers used classical molecular dynamics techniques and polarizable potential models to examine the equilibrium properties such as density profiles and surface tensions of ions at the air/liquid interface of water. They were able to reproduce the experimental surface tensions as a function of the alkali–halide ion-pair, and

they also proposed a molecular model of the distribution of the ions at the air/liquid interface.<sup>8</sup>

In this paper, we present the results of our extensive molecular dynamics simulation of the solvation properties of the  $\text{I}^-$ ,  $\text{Br}^-$ ,  $\text{Cl}^-$ , and  $\text{Na}^+$  ions at the liquid/vapor interface of water. In addition to the above studies, we have also examined the transport mechanism of an  $\text{I}^-$  anion across the water/dichloromethane interface. We believe that this work significantly advances our understanding of molecular processes at the liquid interfaces of water. Our work is distinguished from earlier contributions by the approach and the potential models used and the extent in which we exploited the mean force approach to examine the molecular processes at the interface. The most significant results of the work are the following: (1) We demonstrate that the behavior of these ions at the interface is quite different, and is dependent on the type of anion. The larger  $\text{I}^-$  and  $\text{Br}^-$  anions were found to bind more strongly to the liquid water interface than did the smaller  $\text{Cl}^-$  ion, (2) we compare the PMFs between anions and cations and found that the anions approach more closely to the liquid/vapor interface of water than do the cations, and (3) our computed PMF for transferring an  $\text{I}^-$  anion across the water/dichloromethane interface shows no well-defined minimum near the interface, as in the case of the liquid/vapor interface, but it did show a stabilization free energy of about  $-1$  kcal/mol near the interface with respect to the bulk. In addition, the transport mechanism is quite smooth, and the major energy change occurs when the ion begins to cross the interface. The  $\text{I}^-$  anion was found to carry some water molecules with it as it crossed the interface. A similar results has been observed in the recent experimental studies.<sup>9</sup>

The preliminary results of the study of the interaction of the  $\text{I}^-$  ion with the liquid/vapor interface of water have been published recently.<sup>10</sup> Here, we report a full investigation of the solvation of the  $\text{I}^-$ ,  $\text{Br}^-$ ,  $\text{Cl}^-$ , and  $\text{Na}^+$  ions at the liquid/vapor

<sup>†</sup> I would like to dedicate this work to Professor Peter A. Kollman. I have learned a great deal from you.

**TABLE 1: Potential Parameters for CH<sub>2</sub>Cl<sub>2</sub>, H<sub>2</sub>O, I<sup>−</sup>, Br<sup>−</sup>, Cl<sup>−</sup>, and Na<sup>+</sup> Used in the Molecular Dynamics Simulations<sup>a</sup>**

molecule	atom type	$\sigma(\text{\AA})$	$\epsilon(\text{kcal/mol})$	$q(e)$	$\alpha(\text{\AA}^3)$
CH <sub>2</sub> Cl <sub>2</sub>	C	3.410	0.137	−0.2720	0.878
	H	2.400	0.040	−0.0537	0.135
	Cl	3.450	0.280	0.1897	1.910
H <sub>2</sub> O	H	0.000	0.0000	0.5190	0.000
	O	3.234	0.1825	0.0000	0.000
	M	0.000	0.0000	−1.0380	1.444
I <sup>−</sup>	I	5.1245	0.1000	−1.0000	6.920
Br <sup>−</sup>	Br	4.5436	0.1000	−1.0000	4.770
Cl <sup>−</sup>	Cl	4.3387	0.1000	−1.0000	3.690
Na <sup>+</sup>	Na	2.2718	0.1000	−1.0000	0.240

<sup>a</sup> The potential parameters are taken from refs 11 and 13.  $\sigma$  and  $\epsilon$  are the Lennard-Jones parameters,  $q$  is the atomic charge, and  $\alpha$  is the polarizability.

interface of water as well as the transport mechanism of an I<sup>−</sup> ion across the water/dichloromethane interface. We have also examined the dependence on the size of the anions on the transport mechanism across the liquid/vapor interface. The paper is organized as follows: The polarizable model potentials and the simulation methods are summarized in section II. The results are presented and discussed in section III. Our conclusions and discussion of future research directions are given in section IV.

## II. Potential Models and Computational Methods

**A. Potential Models.** We employ the rigid-body polarizable water model of Dang and Chang to describe the water–water intermolecular interaction.<sup>11</sup> This model describes reasonably well the structure and thermodynamic properties of the bulk and the liquid/vapor interface of water. The total interaction energy of the system is summarized as follows

$$U_{\text{tot}} = U_{\text{pair}} + U_{\text{pol}} \quad (1)$$

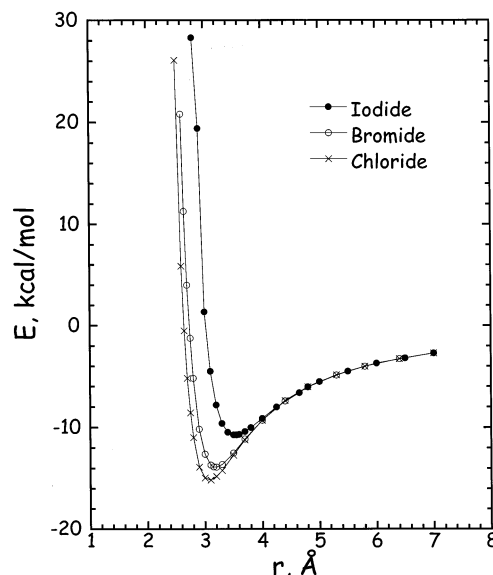
$$U_{\text{pair}} = \sum_i \sum_j \left( 4\epsilon \left[ \left( \frac{\sigma_{ij}}{r_{ij}} \right)^{12} - \left( \frac{\sigma_{ij}}{r_{ij}} \right)^6 \right] + \frac{q_i q_j}{r_{ij}} \right) \quad (2)$$

and

$$U_{\text{pol}} = - \sum_{i=1}^N \mu_i \cdot E_i^0 - \frac{1}{2} \sum_{i=1}^N \sum_{j=1, j \neq i}^N \mu_i \cdot T_{ij} \cdot \mu_j + \sum_{i=1}^N \frac{|\mu_i|^2}{2\alpha_i} \quad (3)$$

Here,  $r_{ij}$  is the distance between site  $i$  and  $j$ ,  $q$  is the charge, and  $\sigma$  and  $\epsilon$  are the Lennard–Jones parameters.  $E_i^0$  is the electric field at site  $i$  produced by the fixed charges in the system,  $\mu_i$  is the induced dipole moment at atom site  $i$ , and  $T_{ij}$  is the dipole tensor. The first term in eq 3 represents the charge–dipole interaction, the second term describes the dipole–dipole interaction, and the last term is the energy associated with the generation of the dipole moment  $\mu_i$ . During molecular dynamics simulations, a standard iterative self-consistent field procedure is used to evaluate the induced dipoles.

The optimized ion–water potential parameters were obtained by running molecular dynamics simulations as previously done to reproduce experimental data such as solvation enthalpies and hydration numbers as well as the data reported from accurate electronic structure calculations for the clusters. The I<sup>−</sup>, Br<sup>−</sup>, Cl<sup>−</sup>, and Na<sup>+</sup> potential parameters are listed in Table 1. In Figure 1, we present the ion–water interaction energy, where we find the minimum energy as a function of orientation for separation distance. The minimum energies were in good agreement with the results obtained from ab initio molecular orbital theory

**Figure 1.** Optimized gas-phase ion–water interaction energies as a function of ion–oxygen separation.**TABLE 2: Structure and Thermodynamic Properties of Ions in Water at 300 K**

ion	$r_{\text{ion-O}}$		coord #		$\Delta H_{\text{sol}}$	
	MD	exp <sup>a</sup>	MD	exp <sup>a</sup>	MD <sup>b</sup>	exp <sup>c</sup>
Na <sup>+</sup>	2.35	2.3–2.4	5.5	5.0–6.0	−100 ± 5	−106
I <sup>−</sup>	3.5	3.5–3.6	6.5	6.0–8.0	−63 ± 4	−64
Br <sup>−</sup>	3.3	3.3–3.4	6.4	7.0–8.0	−76 ± 4	−78
Cl <sup>−</sup>	3.15	3.1–3.2	6.0	6.0–7.0	−78 ± 4	−81

<sup>a</sup> Magini, M. In *Ions and Molecules in Solution*; Tanaka, N., Ohtaki, H., Tamamushi, R., Eds.; Elsevier: Amsterdam 1983 p 97. <sup>b</sup> The solvation enthalpies,  $\Delta H_{\text{sol}}$  are computed by subtracting the total potential energy of the dilute ionic solution from that of pure water. The error bar for the  $\Delta H_{\text{sol}}$  is estimated by taking the difference of the computed  $\Delta H_{\text{sol}}$  from the first half and the last half of the total trajectory. <sup>c</sup> Friedman, H. L.; Krischnan, C. V. In *Water: A Comprehensive Treatise*; Franks, F., Eds. Plenum, New York, 1973, Vol. 1, p 6.

calculations<sup>12</sup> as well as experiments.<sup>13</sup> Furthermore, our calculated interaction energy for Br<sup>−</sup> is very similar to that of Cl<sup>−</sup> and far different from the value calculated for I<sup>−</sup> ion as mentioned above. The computed results of ion solvation in aqueous solution and the experimental data are summarized in Table 2 and Figure 2. From these results, it is clear that our potential model provided an accurate description of the ion–water interactions in solution.

**B. Computational Methodology.** In this study, we used a constrained mean force approach to evaluate the free energies associated with the transfer of an ion across liquid interfaces. The reaction coordinate for ion transfer can be considered to be the  $z_s$  position of the ion. The Helmholtz free energy difference,  $\Delta F(z_s)$ , between a state where the ion is located at  $z_s$ ,  $F(z_s)$ , and a reference state where the ion is at  $z_o$ , is simply

$$\Delta F(z_s) = F(z_s) - F_0 = - \int_{z_o}^{z_s} \langle f_z(z'_s) \rangle dz'_s, \quad (4)$$

where  $f_z(z'_s)$  is the  $z$  component of the total force exerted on the ion at a given  $z$  position, ( $z'_s$ ), averaged over the canonical ensemble. Here,  $F_0$  is chosen as the free energy of the system with the ion located in the bulk water region. During the simulation, the  $z$  coordinate of the ion was reset to the original value after each dynamical step, and the average force acting on the ion was then evaluated. The average forces are

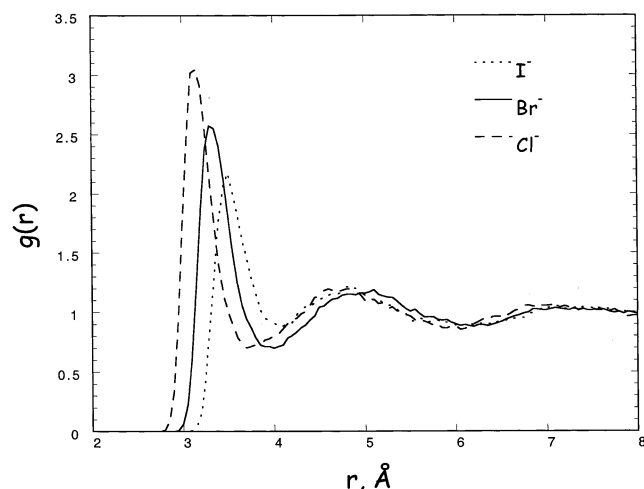


**Figure 2.** Computed radial distribution functions  $g_{I-O}$  ( $I = I^-$ ,  $Br^-$ , and  $Cl^-$ ) near 300 K.

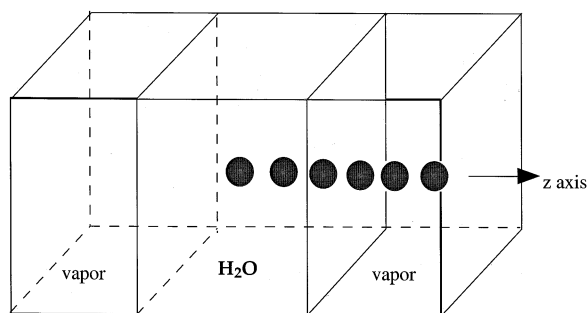


**Figure 3.** Schematic representation of the simulation cell for the transfer of an ion across the liquid vapor interface of water.

subsequently integrated to yield the free energy profile or the PMF. The Z-axis for the ion and the simulation cell are constrained by removing the z-component of the force and the velocity at every step during the molecular dynamics simulation.

The molecular dynamics simulations are performed on a system consisting of an ion and 600 water molecules, in a rectangular simulation cell with linear dimensions of  $26.22 \times 26.22 \times 76.22$  Å (see Figure 3). At the beginning of the simulation, the solute molecule was located at the center of the rectangular cell. The simulations were performed at a constant volume and temperature, with periodic boundary conditions applied in all three directions. The nonbonded interactions (i.e., Lennard-Jones, Coulombic, and polarization) were truncated at molecular center-of mass separations (i.e., water–water and ion–water, interactions were truncated at a molecular separation of 9 Å). During the molecular dynamics simulations, the SHAKE procedure<sup>14</sup> was employed to fix the water geometry by constraining the OH and HH bond lengths. A time step of 2 fs was used in integrating the equations of motion. This approach has been shown to provide comparable results to the reaction field or Ewald summation techniques.<sup>15</sup> For the calculations reported in this paper, the position of the ion ranges from  $z = 0$  to 28 Å, with a position increment of 1.0 Å. The total simulation time at each ion position was averaged over a 300 ps in addition to 100 ps for equilibration. The average forces for a given ion position were converged within a 100 ps simulation time.

### III. Results and Discussion

**A. Liquid/Vapor Interface.** As mentioned earlier, the main thrust of this paper was to characterize mechanism of ion

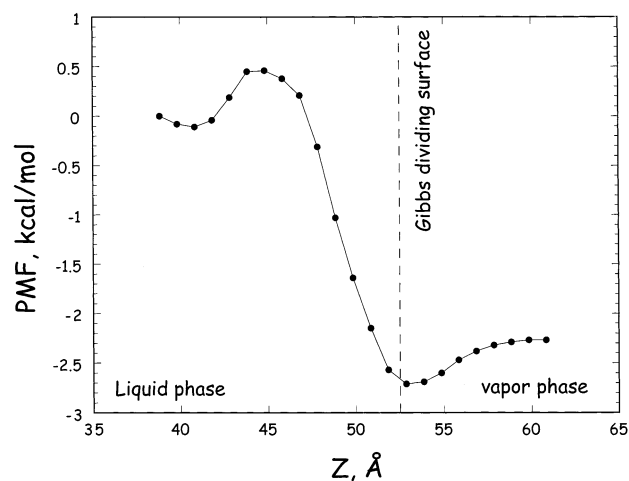


**Figure 4.** Computed free energy profiles for a methane molecule binding to the liquid/vapor interface of water at 300 K.

transport mechanism across the liquid interface of water. We have also used the mean force approach to study the methane–water system, for which experimental data are available.<sup>16</sup> Jorgensen and co-workers had previously studied this system in detail using a free energy perturbation approach.<sup>17</sup> To make the comparison between our results and their results more meaningful, we used their identical pair potential models for methane and water in this study.<sup>18</sup>

In Figure 4, we show the PMF for transferring a methane molecule across the vapor/liquid interface of water at 298 K. It can be seen from Figure 4 that as the methane molecule moves from bulk liquid to the interface, a maximum exists, which indicates that there is a barrier between the bulk solution and the surface-active state. The barrier to dissolution from the liquid water is approximately 0.5 kcal/mol. The existence of such barrier is likely due to the decrease in hydration number of the methane molecule as it begins to approach the interface. The free energy profile then decreases to a minimum that corresponds to a surface-active state in which the methane molecule lies on the face of the surface. The location of the minimum is about 1 Å away from the Gibbs dividing surface (GDS). The free energy profile then increases as the methane leaves the interface to become a gas phase molecule where the mean force is zero and the corresponding PMF is essentially a constant. The hydration free energy estimated from the difference of the gas phase and the liquid-phase free energies is  $2.3 \pm 0.4$  kcal/mol. This result is in excellent agreement with the corresponding experimental measurement<sup>16</sup> of 2.0 kcal/mol and the computed free energy of solvation reported by Jorgensen and co-workers using the free energy perturbation approach.<sup>17</sup> From these results, we conclude that the constrained mean force approach is reliable for use in studies of the ion transport mechanism.

As stated previously, one of the primary focuses of this paper is to elucidate the molecular mechanism of ion binding to the liquid/vapor interface of water at 298 K. The study also characterizes the behavior of these ions at the interface. In Figure 5, we present the free energy profiles for transporting the  $I^-$ ,  $Br^-$ , and  $Cl^-$  ions across the liquid/vapor interface of water. Upon examining these free energy profiles, we made several observations. It is clear that there are two types of interactions between the water interface and these anions. The larger  $I^-$  and  $Br^-$  anions interact more strongly with the interface than the smaller  $Cl^-$  ions. The PMFs of  $I^-$  and  $Br^-$  anions exhibit minima near the GDS with well depths of about  $-1.5$  kcal/mol and  $-0.9$  kcal/mol, respectively. These results are indicative

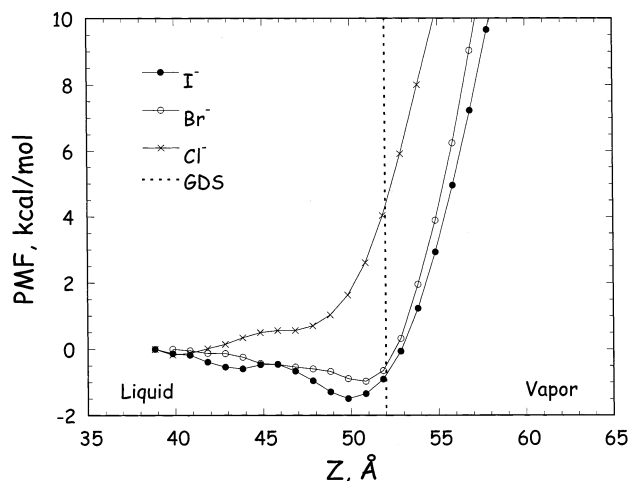


**Figure 5.** Computed free energy profiles for ions binding to the liquid/vapor interface of water at 300 K using polarizable potential models.

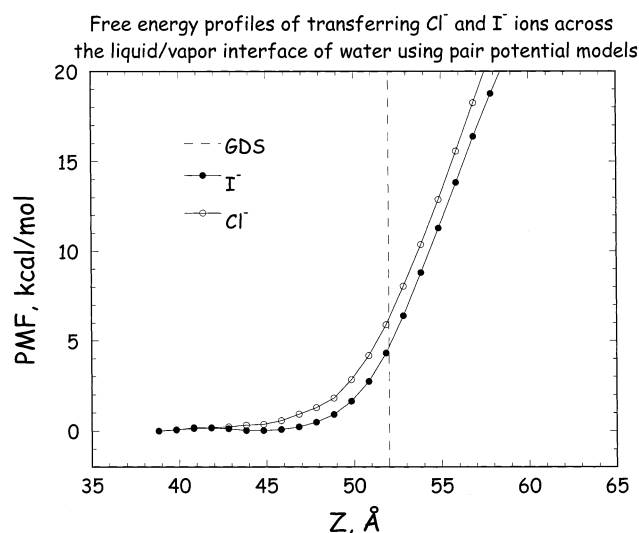


**Figure 6.** Computed free energy profiles for ions binding to the liquid/vapor interface of water at 300 K using pair potential models.

of the stability of the surface state of the polarizable the  $\text{I}^-$  and  $\text{Br}^-$  anions. Furthermore, the physical origin of these results can be explained as follows: when the polarizable iodide or bromide anions are near the liquid/vapor interface of polarizable water, because of the anisotropic solvation, the induced dipole moments of the anions are increased, as well as the total dipole moments of the local water molecules around the anions. Consequently, the ion–dipole induction energies between the anion–water are enhanced due to induction effects.

It is interesting to note that the PMF for the  $\text{Cl}^-$  anion showed no minimum near the water interface, and its PMF is very different to that of the  $\text{Br}^-$  anion. As demonstrated in the above, the gas-phase interactions for  $\text{Br}^-$ – $\text{H}_2\text{O}$  and  $\text{Cl}^-$ – $\text{H}_2\text{O}$  complexes as well as the hydration energies of these ions are nearly identical (see Table 2). To extend our understanding of many-body effects on the transport mechanism, we present in Figure 6, the computed PMFs for the interactions of the nonpolarizable  $\text{Cl}^-$  and  $\text{I}^-$  ions with the liquid/vapor interface of water using pair potential model for water (see ref 18). Upon examination these results; we conclude that the interactions between the anions and the liquid/vapor interface of water are not strongly dependent on the size of the anions. Therefore, the different results in the transport mechanisms of the polarizable ions may be caused by differences in the ion polarizabilities. For instance,

the  $\text{Br}^-$  anion has a polarizability of  $4.77 \text{ \AA}^3$ , which is somewhat bigger than the polarizability of chloride anion of  $3.69 \text{ \AA}^3$ ; and it has been previously demonstrated that the structure of the small ion–water is very sensitive to changes in the ion polarizability.<sup>19</sup> Thus, the PMFs results presented in this paper clearly demonstrate that there is a delicate balance between the anion–water and water–water interactions near the interface. Therefore, the molecular processes at the interface must be modeled with a greater degree of accuracy (i.e., by taking into account more detailed physical processes, namely nonuniform polarization).

The snapshots shown in Figure 7 were taken from the molecular dynamics simulation with the  $\text{Br}^-$  ion located in various positions along the free energy path. As can be seen from Figure 7, the  $\text{Br}^-$  anion carried the hydration shell with it as it left the liquid/vapor interface. Our PMF results are consistent with a most recent simulation study by Jungwirth and Tobias of the distribution of ions in a water slab at a finite concentration.<sup>8</sup> Their computed density profiles for the  $\text{I}^-$  and  $\text{Br}^-$  anions exhibited maxima near the GDS, whereas the computed density profile for the  $\text{Cl}^-$  anion was quite flat. These findings are important because the presence of the  $\text{I}^-$  or  $\text{Br}^-$  ions at the interface could enhance the uptake and/or reactions of the gases, which may have direct physical implications of heterogeneous atmospheric chemistry.<sup>4</sup>

As mentioned earlier, we also computed the PMF for transporting a  $\text{Na}^+$  cation across the water liquid/vapor interface. This study enabled us to investigate the nature of the mechanism for a cation. The simulated results also allowed us to differentiate between the molecular mechanism between the transport of an anion and the cation. In Figure 8, we present the free energy profiles for transporting the  $\text{Na}^+$  cation across the liquid/vapor interface of water. As expected, the PMF for the  $\text{Na}^+$  cation showed no minimum near the water interface, because it has just a small polarizability ( $0.23 \text{ \AA}^3$ ) and its interaction with water is significantly stronger than the ions  $\text{I}^-$ ,  $\text{Br}^-$  and  $\text{Cl}^-$ . For instance, the  $\text{Na}^+$ – $\text{H}_2\text{O}$  interaction energy ( $-24 \text{ kcal/mol}$ ) is quite strong as compared to the corresponding  $\text{Br}^-$ – $\text{H}_2\text{O}$  interaction energy ( $-14 \text{ kcal/mol}$ ). Therefore, we expected a significant difference in the local structures between these solvated ions. Figure 9 illustrates some snapshots taken for various positions of the  $\text{Na}^+$  cation along the free-energy path. As the  $\text{Na}^+$  cation moved from the liquid water interface, it carried a tightly held solvation shells with it as opposite to the loosely held  $\text{Br}^-$ – $\text{H}_2\text{O}$  clusters.

**B. Liquid/Liquid Interface.** We begin this section with a brief discussion of the methods and potential models that are used in this simulation. The study of ion transport across the water/dichloromethane interface is more complicated and more computationally demanding than the case of the liquid/vapor interface of water. The reason for the increased complexity and need for computational resources is that the results are dependent on the balance between ion–water and ion–dichloromethane as well as water–dichloromethane interactions. The potential parameters for the water and dichloromethane<sup>20</sup> interactions were developed recently and the cross interactions between these species were obtained via the Lorentz–Berthelot combining rule.<sup>21</sup> A summary of the  $\text{I}^-$ – $\text{CH}_2\text{Cl}_2$  and  $\text{I}^-$ – $\text{H}_2\text{O}$  interaction energies as a function of ion–molecule separation is shown in Figure 10. The results shown in this figure indicate that the  $\text{I}^-$  ion would prefer to be associated with the aqueous solvent; however, the details of the molecular transport mechanism will have to be mapped out using computer simulation techniques and the mean force approach.



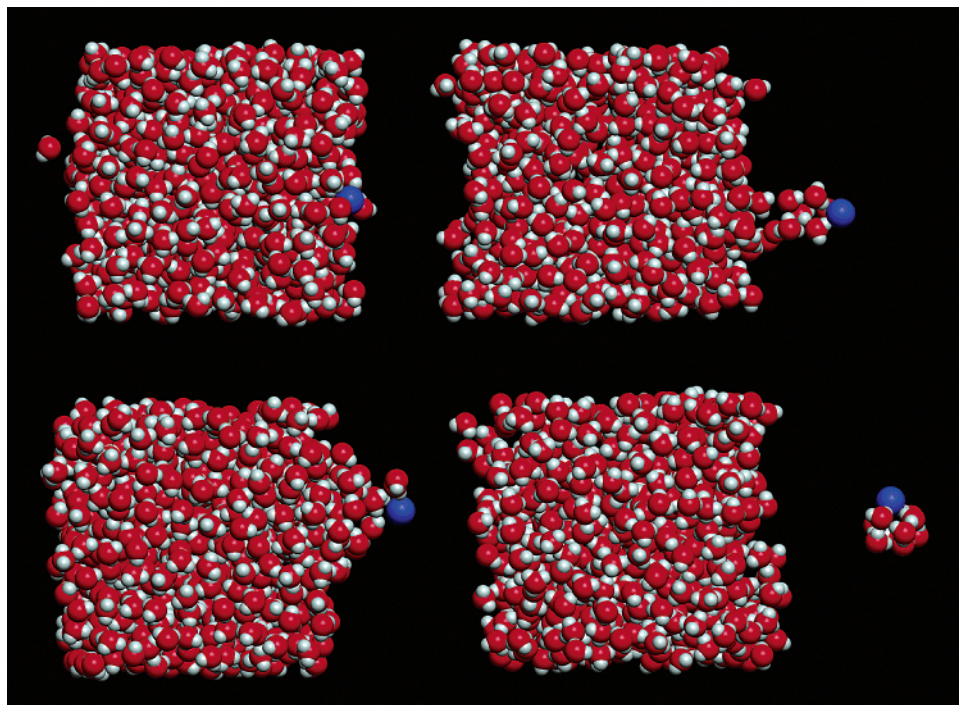


**Figure 7.** Snapshots taken from molecular dynamics simulations using mean force approaches showing the  $\text{Br}^-$  anion leaving the liquid/vapor interface of water.

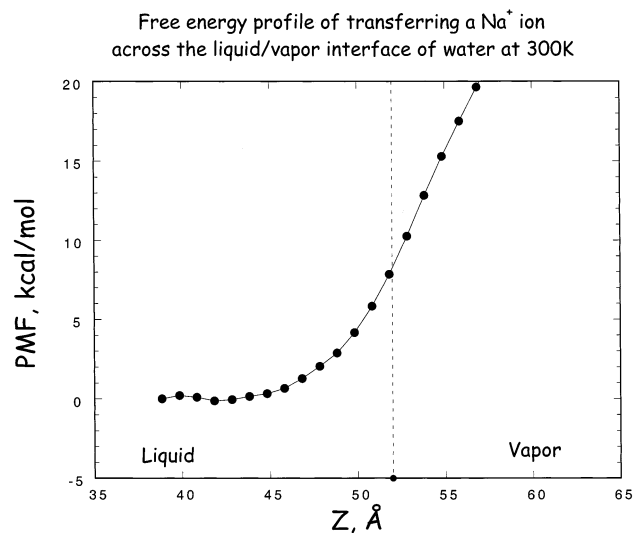


**Figure 8.** Computed free energy profile for transfer an ion  $\text{Na}^+$  across the liquid/vapor interface of water at 300 K.

The details of the simulations are identical to our previous study of the ion transport mechanism across the liquid/liquid interfaces. A brief description of the approach follows.<sup>22</sup> The molecular dynamics simulations are performed on a system consisting of an  $\text{I}^-$ , 1429 water, and 401 dichloromethane molecules in a rectangular simulation cell with linear dimensions of  $35 \times 35 \times 70$  Å. This yields liquid densities of 0.997 and  $1.32 \text{ g/cm}^3$  for water and dichloromethane at room temperature, respectively. The initial configuration of ion transport across the liquid/liquid interface was obtained from previous  $\text{Cl}^-$ |water|dichloromethane simulations. The water molecules are located in the region of  $z > 35$  Å, whereas the dichloromethane molecules occupy the region of  $z < 35$  Å. A total of 28 simulations were carried out to map out the free energy transfer profile. The temperatures of different components (water and dichloromethane) are well equilibrated and maintained around  $300 \pm 4$  K during the simulations. The average forces are

subsequently integrated to yield the free energy profile or the PMF. The position of the ion is constrained by removing the velocity of the iodide anion at every step during the molecular dynamics simulation.

The PMF for transferring an iodide anion across the water-dichloromethane liquid–liquid interface at 298 K as a function of Z-axis normal to the interface is shown in Figure 11. Upon carefully examining the free energy profile, we found that it exhibits a more complicated transfer process as compared to other ions such as  $\text{Cl}^-$  or  $\text{Cs}^+$  ions.<sup>22</sup> We found that there was no well-defined barrier at the liquid/liquid interface as was found in the case of the liquid/vapor interface; however, the computed PMF showed a stabilization free energy of  $-1.0$  kcal/mol as the  $\text{I}^-$  ion approached the liquid/liquid interface. This result indicates that there is a significant probability to find an  $\text{I}^-$  ion near the interface than in the bulk liquid. The computed free energy undergoes major changes as the ion begins to cross the interface. The change in free energy is positive because the  $\text{I}^-$  was shedding the water molecules as it crosses the interface. This result also could be explained by comparing the  $\text{I}^-$ – $\text{H}_2\text{O}$  and the  $\text{I}^-$ – $\text{CH}_2\text{Cl}_2$  dimer potential energy surfaces shown in Figure 10. It is clear that the  $\text{I}^-$  ion prefers the aqueous phase over the nonaqueous phase. The estimated free energy of transfer is  $12. \pm 2$  kcal/mol. There is an experimental measurement of 6 kcal/mol for transferring a single ion  $\text{I}^-$  from the liquid water to the liquid dichloromethane at room temperature.<sup>23</sup> However, the comparison with this experimental data may not be appropriate because our simulated data has indicated that the ion drags some water molecules along with it across the interface.

In addition to the free energy profile, we also calculated the coordination numbers for the  $\text{I}^-$  ion as a function of Z-axis normal to the interface. The computed results indicate that, as the  $\text{I}^-$  ion moves across the interface, its first hydration shell was reduced, due to the competition between  $\text{I}^-$ – $\text{H}_2\text{O}$  and  $\text{I}^-$ – $\text{CH}_2\text{Cl}_2$  interactions. From the calculated PMF and coordination numbers, we concluded that the mechanism of ion transfer involves changes in the hydration shell of the ion. This

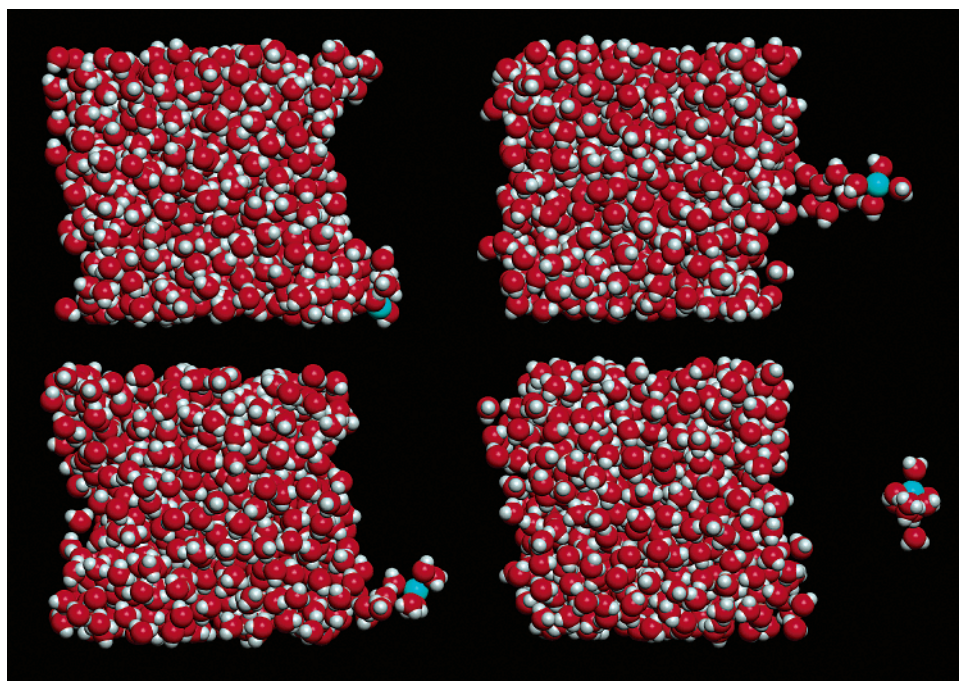


**Figure 9.** Snapshots taken from molecular dynamics simulations using mean force approaches showing the  $\text{Na}^+$  ion leaving the liquid/vapor interface of water.

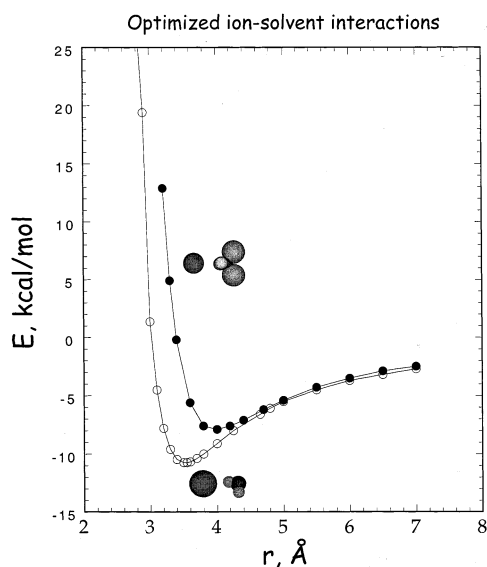


**Figure 10.** Optimized gas-phase  $\text{I}^-$ – $\text{H}_2\text{O}$  and  $\text{I}^-$ – $\text{CH}_2\text{Cl}_2$  interaction energies as a function of ion–molecule separation.

finding is in excellent agreement with a recent experimental study reported by Osakai et al.<sup>9</sup> These authors measured the Gibbs free energy of ion transfer between water and nitrobenzene interface for various ions. For example, the coordination number of a  $\text{Cs}^+$  ion is  $\sim 8$  in water but decreased to  $\sim 1$  when the ion is transferred to nitrobenzene. In Figure 12, snapshots were taken from the molecular dynamics simulation for various positions of the  $\text{I}^-$  ion in the  $\text{CH}_2\text{Cl}_2$  liquid phase. As can be seen, the features of our results are very close to the model suggested by Osakai et al.<sup>9</sup>

#### IV. Conclusion

In this study, we carried out extensive molecular dynamics simulations of the solvation properties of the  $\text{I}^-$ ,  $\text{Br}^-$ ,  $\text{Cl}^-$ , and  $\text{Na}^+$  ions at the liquid/vapor interface of water. We demonstrated that these ions behave differently at the interface, depending

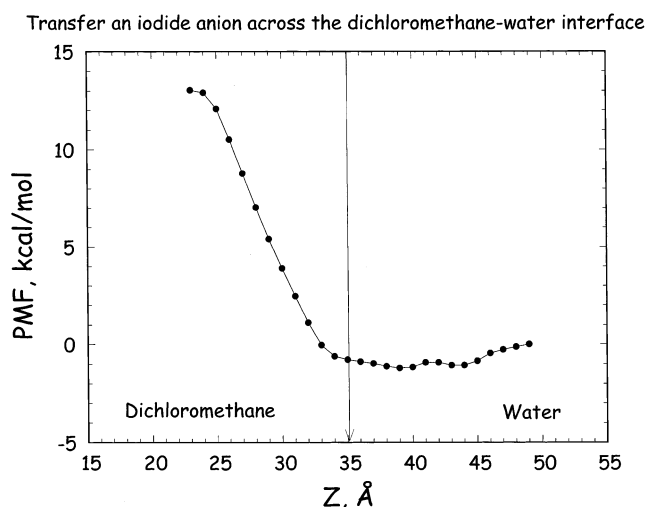


**Figure 11.** Computed free energy profile for transfer an  $\text{I}^-$  ion across the water-dichloromethane liquid/liquid interface at 300 K.

on the type of anion. The larger  $\text{I}^-$  and  $\text{Br}^-$  anions were found to bind more strongly to the liquid water interface than the smaller  $\text{Cl}^-$  ion. We also compared the PMFs between anions and cations and found that the anions approach more closely to the liquid/vapor interface of water than cations. We note that many computed results such as the comparison of  $\text{Cl}^-$  and  $\text{Br}^-$  ions in the gas phase and at the liquid/vapor interface, are presented for the first time. We hope that the present contribution will stimulate further experimental work in the area.

We also studied the mechanism for transporting an  $\text{I}^-$  ion across the water/dichloromethane interface. Our computed PMF for this transfer showed no well-defined minimum near the interface, as in the case of the liquid/vapor, but it did show a stabilization free energy of about  $-1$  kcal/mol near the interface with respect to the bulk liquid. In addition, the transport mechanism appears to be quite smooth and the major energy change occurred when the ion began to cross the interface. The  $\text{I}^-$  ion was found to carry some water molecules with it as it



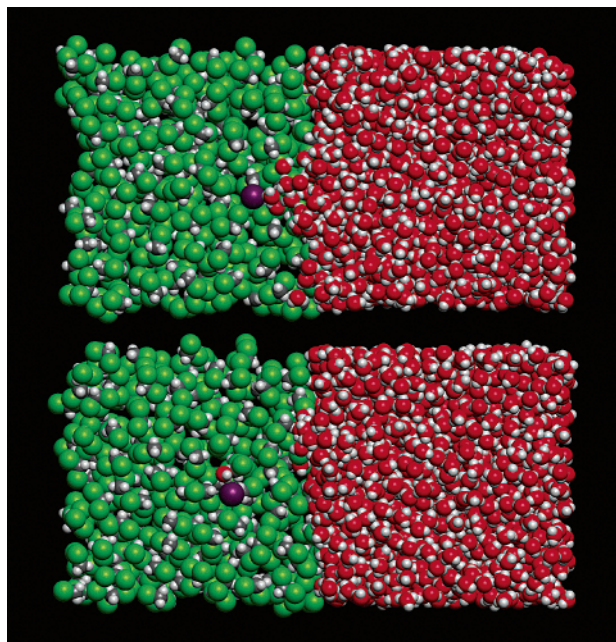


**Figure 12.** Snapshots taken from molecular dynamics simulations using mean force approaches showing the  $\text{I}^-$  ion moving along the free energy path of the liquid/liquid interface near 300 K.

crossed the interfaces. A similar observation from an experimental study has been reported.

These results have demonstrated that the computer simulation technique used in conjunction with the potential of mean force approach can be successfully applied to the study of a variety of chemical and physical problems. Our work is not only able to compare to the experimental data, it also provides a detailed physical description of the molecular mechanism for transport of ions across the liquid interface of water. In addition, our work differs from earlier contributions in that our potential models have taken into account many-body effects, as it has been demonstrated previously that, in some cases, these effects cannot be neglected.<sup>19</sup>

**Acknowledgment.** This work was performed in the William R. Wiley Environmental Molecular Sciences Laboratory (EMSL)

at Pacific Northwest National Laboratory (PNNL) under the auspices of the Division of Chemical Sciences, Office of Basic Energy Sciences, U.S. Department of Energy. PNNL is operated by Battelle for the Department of Energy. Computer resources were provided by the Division of Chemical Sciences and by the Scientific Computing Staff, Office of Energy Research, at the National Energy Research Supercomputer Center (Berkeley, California). Operation of EMSL is supported by DOE's Office of Biological and Environmental Research.

## References and Notes

- (1) *Biophysics of Water*; Franks, Mathias, S., Eds.; Wiley-Interscience: New York, 1982.
- (2) McLaughlin, S. *Annu. Rev. Biophys. Biophys. Chem.* **1989**, *18*, 113.
- (3) Honig, B.; Hubbell, W. L. and Flewelling, R. F. *Annu. Rev. Biophys. Biophys. Chem.* **1986**, *15*, 163.
- (4) Knipping, E. W.; Lakin, M. J.; Foster, K. L.; Jungwirth, P.; Tobias, D. J.; Gerber, R. B.; Daddub, D.; Finlayson-Pitts, B. *Science* **2000**, *288*, 301, and references therein.
- (5) Haag, W. R.; Yao, C. C. D. *Environ. Sci. Technol.* **1992**, *26*, 1005; US Department of Energy, Office of Environmental Management, FY 1995 Technology Development Needs Summary, 1994; p 2–17.
- (6) Wilson, M. A.; Pohorille, A. *J. Chem. Phys.* **1991**, *95*, 6005.
- (7) Schweighofer, K. J.; Benjamin, I. *Chem. Phys. Lett.* **1993**, *202*, 379; *J. Phys. Chem.* **1999**, *103*, 10 274.
- (8) Jungwirth, P.; Tobias, D. J. *J. Phys. Chem. B* **2001**, *105*, 10 468.
- (9) Osakai, T.; Ogata, A.; Ebina, K. *J. Phys. Chem. B* **1997**, *101*, 8341.
- (10) Dang, L. X.; Chang, T–M. *J. Phys. Chem. B* **2002**, *106*, 235.
- (11) Dang, L. X.; Chang, T–M. *J. Chem. Phys.* **1997**, *106*, 8149.
- (12) Xantheas, S. *J. Phys. Chem.* **1995**, *100*, 9703.
- (13) Hiraoka, K.; Mizuse, S. and Yamabe, S. *J. Phys. Chem.* **1988**, *92*, 3943. (b) Arshadi, M.; Yamdagni, R.; Kebarle, P. *J. Phys. Chem.* **1970**, *74*, 1475.
- (14) H. J. C. Berendsen, H. J. C.; Postma, J. P.; Di Nola, A. Van Gunsteren, W. F.; Haak, J. R. *J. Chem. Phys.* **1984**, *81*, 3684; Ryckaert, J. P.; Ciccotti, G. and Berendsen, H. J. C. *J. Comput. Phys.* **1977**, *23*, 327.
- (15) Perara, L.; Essmann, U.; Berkowitz, M. *J. Chem. Phys.* **1995**, *102*, 450; Spohr, E. *J. Chem. Phys.* **1997**, *107*, 6342.
- (16) Ben-Naim A. and Marcus, Y. *J. Chem. Phys.* **1992**, *96*, 4712.
- (17) Jorgensen, W. L. *Chem. Phys.* **1983**, *79*, 926.
- (18) Jorgensen, W. L., Chandrasekhar, J.; Madura, J.; R. W. Impey, R. W.; Klein, W. L. *J. Chem. Phys.* **1983**, *79*, 926.
- (19) Dang L. X., Smith, D. E. *J. Chem. Phys.* **1993**, *99*, 6950.
- (20) Dang L. X. *J. Chem. Phys.* **1999**, *100*, 10 122.
- (21) Hansen J. P.; McDonald, I. R. *Theory of Simple Liquid*; Academic: London, 1986.
- (22) Dang L. X. *J. Phys. Chem. B* **2001**, *105*, 804.
- (23) Marcus, Y. *Pure Appl. Chem.* **1983**, *55*, 977.